Turbulent Airfoils for General Aviation

Richard Eppler*
Universität Stuttgart, Federal Republic of Germany

Several new airfoils are presented which have short pieces of steep favorable pressure gradient followed by an early pressure recovery which is a compromise between the Stratford distribution and soft stall. The drag polars are computed by a mathematical model, which is briefly described. For comparison, NACA 65_2-415 and NASA GA(W)-1 airfoils are evaluated using the same model; in this case the results are also compared with experimental drag polars.

I. Introduction

EXCEPT for a few examples,[1,2] general aviation airplanes do not exploit laminar boundary layer flow. It is doubtful that this is an optimal approach since examples of effective airfoils have been published[3] and fuel prices are increasing. But also without using laminar airfoils it is more important today to replace engine power by aerodynamic drag reduction. This can be achieved by airfoils allowing good take-off and landing with higher wing loading and hence smaller wing area, while drag under cruising conditions is reduced as far as possible. Airfoil thickness is significant in order to obtain higher aspect ratios and/or lower wing weight. Recently considerable progress in this direction has been made by the airfoil GA(W)-1.[4] In the present paper a continuation of this work is discussed and it is shown that certain improvements are possible.

II. Mathematical Model

In this paper all comparisons between different existing and new airfoils are made using a mathematical model, for which a FORTRAN program exists. Such "computer wind tunnels" are much cheaper and are sufficient for comparison purposes. Of course, they should be supplemented by wind-tunnel tests and, even more important, by free-flight measurements. The computer program used here is similar to the program described in Ref. 5. The differences are described below.

A. Potential Flow

For the calculation of the potential flow there are two options available. The first one is a conformal mapping method for airfoil design based on the properties of the pressure distribution as described in Refs. 6-8. The second one is a panel method for the airfoil analysis problem as used in Ref. 5. Special, curved singularity elements with linear vorticity distribution have been developed in order to obtain good results near the trailing and leading edge and for thin airfoils. The distribution of the points on the airfoil surface is arbitrary. Thus it was possible to use the analysis program for many airfoils designed by the design routine. The panel method calculations show very small differences from the results as obtained from conformal mapping, mainly in the lift curve slope. The deviation is decreasing with increasing number of points and negligible for all applications in this paper.

B. Boundary-Layer Method

With the potential flow methods the pressure distribution around an airfoil for every arbitrary angle of attack can be obtained. The pressure distribution together with a Reynolds number Re specifies a boundary-layer flow around the airfoil. The approximative method which is used here to calculate the boundary-layer flow is published in Ref. 9. This calculation yields the momentum thickness $\delta_2(s)$ and the shape parameter $H_{32}(s)=\delta_3/\delta_2$ dependent on the arc length s from the stagnation point, where δ_3 is the energy thickness of the boundary layer. The method is, like many others, based on the momentum and energy equations for the entire boundary-layer thickness. For boundary-layer transition an empirical criterion for the local Reynolds number, $Re_{\delta_2}=(U/U_\infty)(\delta_2/c)Re$, is used, where U is the local potential flow velocity, U_∞ is the freestream velocity, and c is the chord length. Transition is assumed to occur, if (Fig. 1)

$$Re_{\delta_2} \geq Re_T = 18.4H_{32} - 21.74 - 0.36r$$

Here r is a "roughness degree;" $r=0$ means smooth surface and undisturbed freestream; for $r=4$ the criterion gives much earlier transition as it may occur at rough surface and/or in

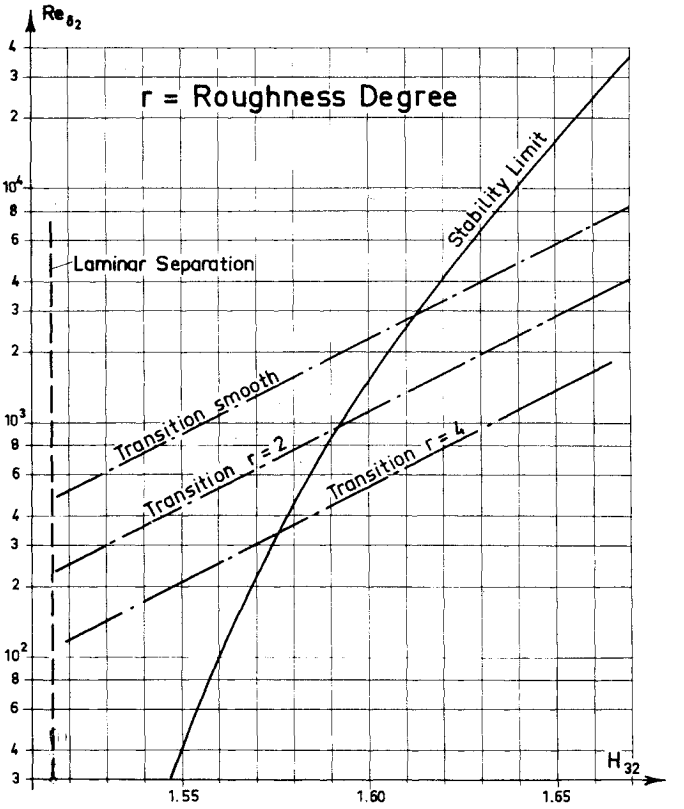

Fig. 1 Transition criteria.

Received July 13, 1976; revision received Feb. 25, 1977.

Index category: Aircraft Aerodynamics.

*Professor, Mechanics.

very turbulent freestream. The values $1 \leq r \leq 3$ can be used for intermediate degrees of disturbance. In this model, the roughness degree r influences only the location of the boundary-layer transition. Any influence of roughness on the boundary-layer development is not taken into consideration.

In Ref. 3 this transition criterion was introduced and tested for $r=0$ by comparing the numerical results with experimental measurements, where reasonable agreement was obtained. It would not be difficult to also introduce amplification integration criteria as presented in Ref. 10. However, such criteria are empirical also since there is no information on the original disturbance level, and since some waves are first unstable and later stable, when others become unstable. Since more computional effort is required when using amplification integration, it has not yet been introduced in the program system. It may be surprising that for $H_{32} > 1.62$ the transition line is below the linear stability limit. Such H_{32} values can only be reached by suction. However, suction is normally combined with finite disturbances, for which the linear stability theory is not applicable. For this reason suction experiments have indeed shown that transition mostly occurs before the linear stability limit is reached. It should be remarked that it is helpful to plot the boundary layer results $H_{32}(s)$ and $\delta_2(s)$ in the coordinates of Fig. 1 if the transition and separation danger is to be judged.

Concerning local laminar separation or separation bubbles,[11,12] the boundary-layer method[9] shows a certain analogy to the bubbles, and so far it was possible to avoid bubbles in the real flow application by avoiding the analogy in the mathematical model. This can be done by implementing after transition a so-called transition ramp, i.e. a region of moderate adverse pressure gradient. The length of this region and the magnitude of this pressure gradient is dependent on Reynolds number.

C. Total Lift and Drag

After the boundary-layer results $\delta_2(s)$ and $H_{32}(s)$ are available for various angles of attack, the next step must be to determine the total lift and drag.

The potential theory described in Sec. IIA yields for an airfoil the direction of zero lift as well as the lift curve slope $\partial c_l / \partial \alpha$, and hence for arbitrary angles of attack a lift coefficient c_l can be obtained. The boundary-layer results allow for arbitrary angles of attack the adding of the displacement thickness to the airfoil shape; then the analysis program can be used again for the new shape.[5] Thus a new pressure distribution and a new lift coefficient can be calculated. It could be considered to use the new pressure distribution for another boundary-layer calculation and new displacement iterations.

The results of such an iteration are not valid when boundary-layer separation has occurred, which has much more effect on the lift coefficient than displacement. Therefore the mathematical model uses no displacement iteration. In a kind of an engineering approach, without separation the lift curve slope is taken 2π, while potential theory gives a somewhat higher value for airfoils with finite thickness. This fact corresponds to practical experience, where for airfoils which are not too thin the gain in the lift curve slope by finite thickness is approximately lost again by displacement effects, when separation does not occur.

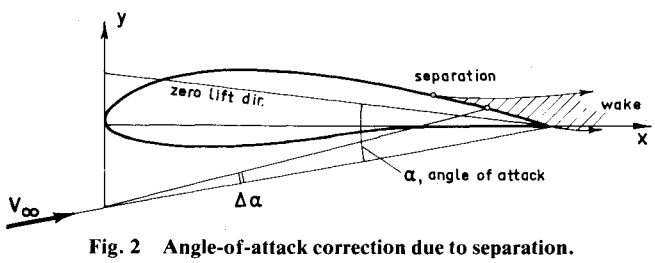

Fig. 2 Angle-of-attack correction due to separation.

It seems to be more important to account for the effect of separation on the lift coefficient. This is done by an additional loss of angle of attack $\Delta\alpha$ as sketched in Fig. 2. The value of $\Delta\alpha$ is defined by replacing the trailing edge by the midpoint between separation point and trailing edge. This approach is not as crude as it may appear at first. A detailed justification for this approach is given by the potential theory of wake flow.[13] However, the influence of separation on the potential flow pressure distribution and again on separation is not taken into consideration.

The total drag coefficient can be derived from the shape parameter and the momentum thickness at the trailing edge using the formulas of Squire-Young and of Betz.[14,15] For wakes with very small differences from the freestream, both formulas asymptotically give the same results. However, the results differ and are both not exact for strong wakes, which occur after boundary-layer separation. Already, for boundary layers not yet being separated but near separation (low H_{32}, high H_{12}) at the trailing edge, the formulas are problematic. Therefore NASA suggested a modification of the Betz formula to be used in a NASA mathematical model.[16] In the model used for this paper, a modification of the Squire-Young formula

$$c_d = 2\frac{\delta_{2T}}{c}\left(\frac{U_\infty}{U_T}\right)^{(5+H_{12T})/2}$$

was introduced, where index T refers to the "trailing edge." With

$$H_{12T} = 2.5 \quad \text{if} \quad H_{12T} > 2.5$$

where $H_{12} = \delta_1/\delta_2$ and δ_1 = displacement thickness, results are obtained which are very close to those obtained from the NASA formula.

All formulas start from δ_2 at the trailing edge δ_{2T}. No influence of separation on the drag is considered. This is not too bad, because separation does not increase δ_{2T} directly. Also, potential wake theory[13] shows that there is no direct influence of the wake on the drag as long as the velocity at separation is smaller as the freestream velocity. Thus the pure friction drag should be a reasonable approximation for the total drag as long as separation does not occur too early. It is rather peculiar that the model shows rapidly increasing friction drag if the separation distance from the trailing edge increases. Further, even near the maximum lift the results are not completely wrong.

D. Example

The airfoil NACA 64_2-415 is used as an example for the application of the mathematical model and for comparison with wind tunnel results.[17] In Fig. 3 the potential flow velocity distribution is plotted for four angles of attack. The analysis program uses the original coordinates published in Ref. 17. On both sides one additional point was splined in between $x/c=0.9$ and $x/c=0.95$, and two points between $x/c=0.95$ and $x/c=1.0$.

Figure 4 shows the $c_d - c_l$ polar for $Re=3.10^6$ and $Re=9.10^6$ for smooth conditions ($r=0$) and for $Re=6.10^6$ with transition mode $r=4$ (rough conditions). The wind tunnel results of Ref. 17 are shown in the same diagram.

Some comments on the results are presented as follows:

1) The NACA 6 series objective is such that the velocity difference between upper and lower surface should be constant for $\alpha=0$. This is realized except near the leading and trailing edge. The design lift coefficient $c_{li}=0.4$ (fourth digit in airfoil number) is thus reduced to $c_{li}=0.36$.

2) The laminar bucket should be symmetrical to the design lift coefficient. Figure 3 shows that this is not realized in the potential flow. The lower surface has a much higher suction peak for $\alpha=-3$ deg than the upper surface for $\alpha=+3$ deg. This is due to the approximative handling of camber by

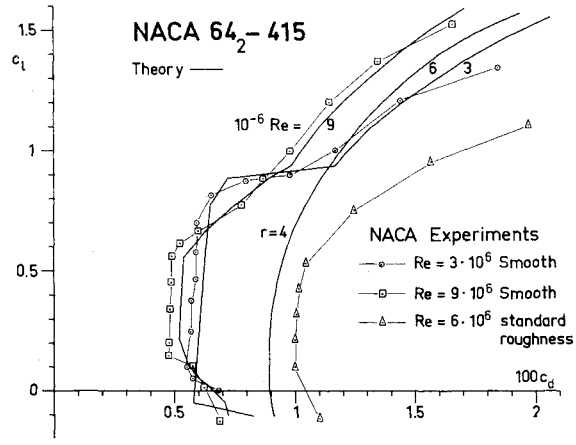

Fig. 3 NACA 64_2-415 airfoil with potential flow velocity distributions.

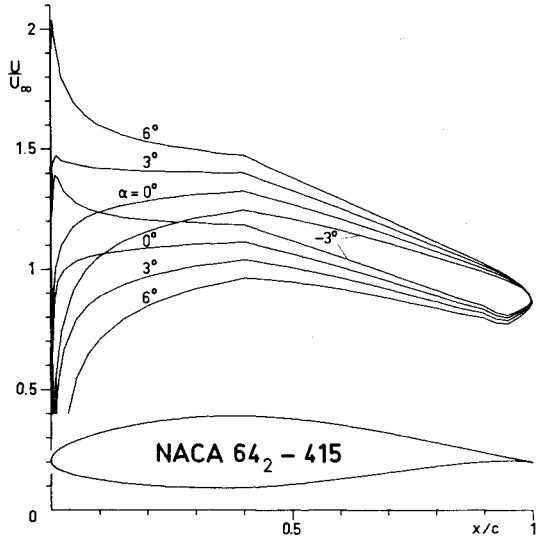

Fig. 4 NACA 64_2-415 $c_d - c_l$ polars.

centerline singularities in the development of the NACA 6-series airfoils.

3) Near the lower end of the laminar bucket the mathematical model is very sensitive to small changes. Splining in one additional point on both sides of the leading edge has no noticeable influence to the potential flow distribution. However the lower end of the laminar bucket for $Re = 3.10^6$ is shifted upwards from $c_l \approx -0.1$ to $c_l \approx 0$. It must be concluded that in the experiments the lower end of the laminar bucket is also sensitive to the exact shape of the model. Therefore it is not surprising that in all comparisons which have been made so far the upper end of the laminar bucket agrees better with experiments than the lower end. The latter even deviates in different directions for different airfoils. For NACA $64_2 - 415$, the experimental laminar bucket ends earlier (at a higher c_l) than the theoretical one. For other airfoils the opposite is true.

4) For $Re = 3.10^6$, the theoretical transition point at both ends of the laminar bucket suddenly moves from $x/c \approx 0.4$ to the leading edge, and the laminar bucket in the $c_d - c_l$ polar ends abruptly on both sides. The same evidence has been observed in the experiments. The explanation for this is clearly given by the potential flow distribution. For increasing α, a suction peak is arising at the upper surface near the leading edge, and for decreasing α at the lower surface. It can be shown that this is due to the philosophy of the 6-series airfoils for which constant velocity for a certain α is obtained at each side. The nonexact handling of the leading edge intensifies this feature. For $Re = 9.10^6$ the theory shows that the transition point is moving slowly towards the leading edge, the laminar bucket is smaller and the ends are less abrupt. This feature is also observed in the experiments.

5) Also, the theoretical lift and drag values outside of the laminar bucket are not completely wrong in comparison to the experiments and even the $c_{l\max}$ values (not shown here) do not compare too badly. It should be stated that these values are also a little problematic in the experiments.

6) The absolute values of the smooth-condition theoretical drag coefficients are, in Fig. 4, about 10-15% higher than the experimental results. The same difference occurs in all comparisons with NACA results[17] which have been performed so far. It would not be difficult to adapt the skin friction law in the boundary layer method to these experiments. Since comparisons with measurements in other wind tunnels show different tendencies, no adaption was tried so far. With $r = 4$ (rough condition transition mode) the theoretical c_d values are less than the standard roughness measurements given in Ref. 17. It must be concluded that this standard roughness not only causes transition, but also increases skin friction considerably in the turbulent boundary layer. This is not surprising, as the standard roughness consists of 0.011-in. carborundum grains and "is considerably more severe than that caused by the usual manufacturing irregularities or deterioration in service" (Ref. 17, p. 24).

Summarizing the example (and many more experiences) shows that the mathematical model is adequate for comparison of different airfoils. It is probably more adequate for comparison purposes than comparing results from different wind tunnels. The absolute values of c_d inside the laminar bucket are problematic, but this could be also true for wind-tunnel results.

E. Stall Characteristics

If, near maximum lift, c_l decreases more or less unsteadily with increasing α, the airfoil is said to have hard stall. There are several reasons for the occurrence of the so-defined hard stall. The mathematical model realizes two of them: 1) an unsteadily moving transition point can change the initial conditions of the pressure recovery such that the turbulent separation is also moving unsteadily; or 2) the turbulent separation is moving rapidly due to other reasons. This occurs mainly if, for a certain α,[18] the turbulent boundary layer approaches the so-called Stratford distribution[19] which is near separation over a wide range. In this case, increasing α and increasing adverse pressure gradient also cause a fast-moving turbulent separation point. Needless to say, the Stratford distribution is also very sensitive to initial conditions.

So far, it has been possible to obtain soft stall in real flow by preventing hard stall in the mathematical model. This implies that unsteady motions of the transition point must be prevented. Concave pressure recovery functions as suggested in Ref. 20 should be used, but in the beginning they should not be nearly as steep as the Stratford distribution.

III. The GA(W)-1 Airfoil

It has recently been found that the airfoils for normal general-aviation aircraft can be improved by using the mathematical models and computer programs available today. A successful airfoil, GA(W)-1, was presented in Ref. 4. The philosophy of this development was to agree with rough surfaces and to optimize other features of the airfoil such as maximum lift coefficient and stall characteristics. The drag reduction could then be achieved by using smaller wings. Thus, this airfoil has a large leading-edge radius and a large degree of camber near the trailing edge. In the NASA measurements this intention was realized very well.

It is always very informative to also analyze an experimentally tested airfoil in the computer. In Fig. 5, four

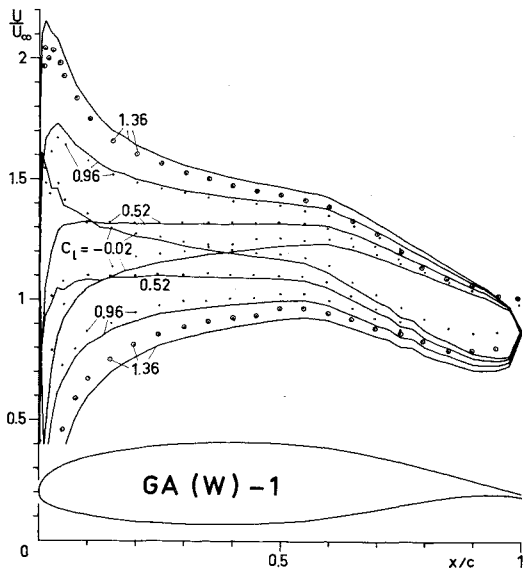

Fig. 5 NASA GA(W)-1 airfoil with potential flow velocity distributions.

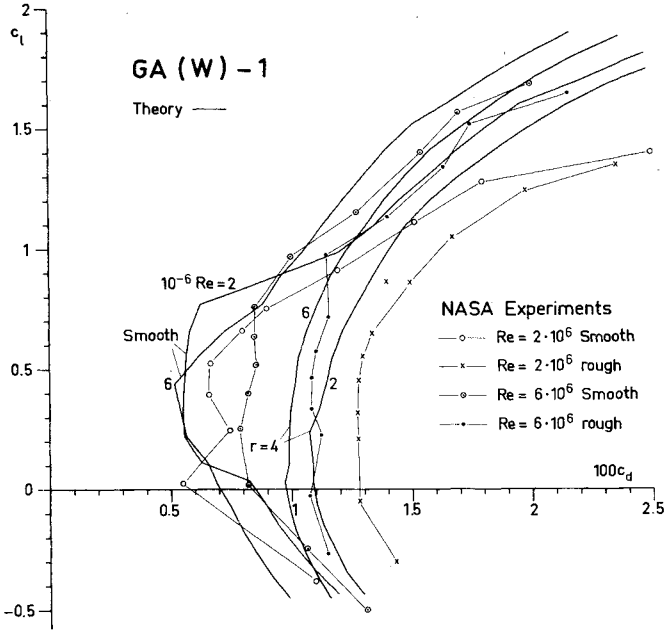

Fig. 6 NASA GA(W)-1 $c_d - c_l$ polars.

potential flow velocity distributions are presented. They have, with a 2π lift curve slope, the same c_l as the experimental distributions in Ref. 4. The agreement between theory and experiment is good. Both show clearly the philosophy of this airfoil: 1) a blunt leading edge preventing high suction peaks up to high angles of attack, 2) no angle of attack with long favorable pressure gradient simultaneously on both sides, and 3) earlier and (related to minimum c_p) more pressure recovery at the lower surface than at the upper one.

Near the trailing edge the upper surface potential flow has a short piece of high adverse pressure gradient which causes a short separation in viscous flow. The same is true for all NACA 6 series airfoils with the $a = 1$ mean line, for some of the airfoils presented here and many others. In Ref. 17 it was shown already that this separation has very little effect. It is far smaller than the effect of the restriction that the upper and lower surface must already have the same velocity 5 or 10% in front of the trailing edge, as was introduced by H. Liebeck.[18] Even there the potential flow adverse pressure gradient near the trailing edge is not eliminated. It is present due to the finite trailing edge angle and due to the stagnation point at the trailing edge. The only difference to GA(W)-1 is that the adverse pressure gradient is (for a certain angle of attack) the same at the upper and lower surface.

Figure 6 shows the theoretical and experimental $c_d - c_l$ polars for $Re = 2.10^6$ and $Re = 6.10^6$, for smooth and rough conditions respectively. Both theoretical and experimental results clearly demonstrate the success of this airfoil. It has very high $c_{l\max}$, even for rough conditions, and a moderate $c_{d\min}$. In detail, for $Re = 2.10^6$ there exists a considerably large laminar bucket. For $Re = 6.10^6$ only the theoretical line for smooth conditions has a small laminar bucket. Unlike Fig. 4, the theoretical c_d values are smaller than in the experiments. All that agrees with the information obtained from Mr. Pierpont, NASA Langley Research Center,[21] that the wind tunnel used for the GA(W)-1 experiments did not yet have the low turbulence level which it had for the former NACA measurements. The NASA standard roughness applied for GA(W)-1 is much less than the NACA standard roughness in Ref. 17. Therefore, the transition mode $r = 4$ has a similar effect. For high c_l, the theory leads to much smaller c_d than the experiments. Here the theory is problematic since it does not account for the form drag. Since in other comparisons with experiments the difference is smaller, one could imagine that certain problems also arise when measuring high lift coefficients between fixed tunnel walls.

IV. New General-Aviation Airfoils

The results presented so far suggest an application of the mathematical model for comparisons between new sections to be designed and existing airfoils. It can be expected that an airfoil which is better with respect to the mathematical model will have advantages in practical applications. Wind-tunnel and free-flight tests should supplement this procedure. Since they are much more expensive, they could be restricted to a few representative examples. The philosophy concerning the GA(W)-1 airfoil may be continued. The mathematical model allows the tailoring of airfoils for every special application. The direction in which this tailoring may go can be best demonstrated with a few examples.

Many applications have similar requirements. The most important flight conditions and their requirements are:

1) Cruise – minimized total airplane drag.

2) Takeoff and landing – certain requirements for minimum flap-down speed must be met. Higher flap-down maximum lift coefficient allows smaller wing area.

3) Climb – maximized maximum c_l^3/c_d^2 for the entire airplane.

Normal general-aviation airplanes have low aspect ratios. The minimum sinking speed normally occurs at lift coefficients of about 0.5 to 0.6; hence high lift coefficients are not necessary for climb conditions. They are much more influenced by the span than by any airfoil data. Therefore, a higher relative thickness of an airfoil, which allows the above-mentioned wing area reduction in chord direction, is important for climbing conditions. Moreover, thick airfoils allow higher structures and again less chord, and thus not only lead to less wing surface drag but also to less interference drag under cruise conditions.

For conditions 1 and 2, the following philosophy seems to be reasonable, if a smooth surface is not intended:

1) Near the leading edge a short piece of very favorable pressure gradient should exist, which allows a laminar boundary layer in spite of a rough surface.

2) Any sudden movement of the transition and separation location must be prevented.

3) After transition the pressure recovery should begin as early as possible. Concerning drag, the Stratford pressure distribution[19] would be the optimum. But this distribution on the upper surface would lead to very hard stall. Thus a distribution is applied, which initially is not nearly as steep as

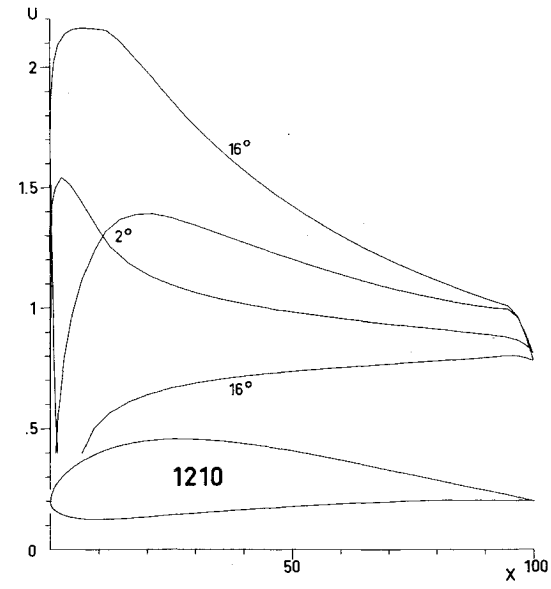

Fig. 7 Airfoil 1210 with potential flow velocity distributions.

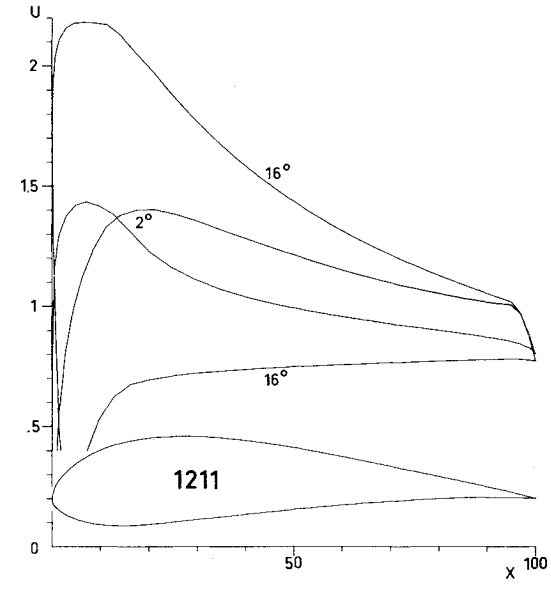

Fig. 9 Airfoil 1211 with potential flow velocity distributions.

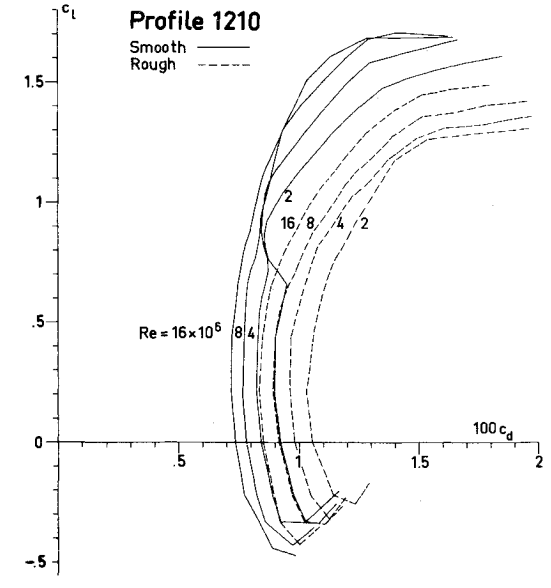

Fig. 8 $c_d - c_l$ polars for airfoil 1210.

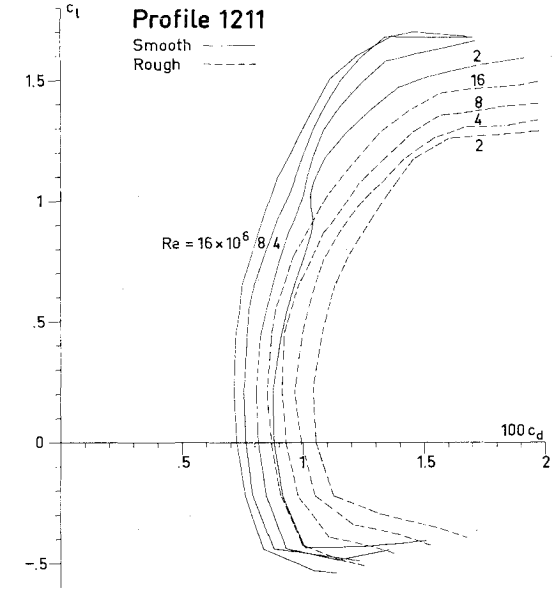

Fig. 10 $c_d - c_l$ polars for airfoil 1211.

the Stratford distribution, but which almost gives the same recovery and drag values in combination with higher lift and very soft stall.

A first airfoil 1210 with some typical velocity distribution is shown in Fig. 7 (α is always measured from the direction of zero lift). For cruise conditions ($\alpha = 2$ deg, $c_l = 0.22$), the velocity distribution of the upper surface has a very favorable pressure gradient until $x = 10\%$. For a large angle of attack of $\alpha = 16$ deg ($c_l = 1.76$ without separation) this shape leads to a rather flat distribution without a suction peak. For $\alpha = 16$ deg, the shape of the pressure recovery is specified concave as mentioned, but not nearly as extreme as the Stratford distribution. At the lower surface the region of favorable pressure gradient is smaller and the pressure recovery is steeper. For reversed flight a soft stall is not necessary.

The computer drag polars for smooth and rough ($r = 4$) conditions are shown in Fig. 8. For smooth conditions and lift coefficients $c_l \approx 0.6$, depending on *Re*, the boundary layer on the lower surface becomes laminar. The drag is not very much reduced. Of course, no laminar bucket exists. It is impossible that both sides have a long laminar boundary layer, as is true for airfoil GA(W)-1 at lower Reynolds numbers. However, both airfoils are not intended for smooth-surface applications. They must be compared for rough conditions, $r = 4$. Now, for nearly all positive lift coefficients airfoil 1210 is better than airfoil GA(W)-1. Only the maximum lift coefficient of the GA(W)-1 is somewhat higher. On the other hand, airfoil 1210 has a lower moment coefficient and is less aft-loaded, as can be seen from Figs. 5 and 7. Allowing the same moment coefficient, the same maximum lift coefficient could be achieved. But this does not seem to be an important feature, since flaps are used for takeoff and landing. A more important difference between the two airfoils concerns the thickness; airfoil 1210 has 15.8%, while airfoil GA(W)-1 has 17.0% thickness.

Therefore the next modification concerns the thickness. Profile 1211 (Fig. 9) has exactly the same specifications for the upper surface, but on the lower side we have a larger region of favorable pressure gradient and therefore more pressure recovery, which is again more Stratford-like than on the upper surface. The thickness is now 18.0%.

Figure 10 shows the computed drag polars. For smooth conditions, the laminar effects of the lower surface are shifted towards higher c_l values and these effects are also smaller.

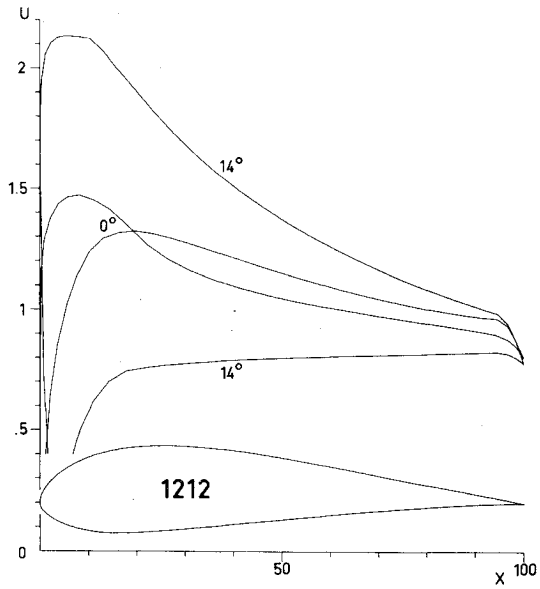

Fig. 11 Airfoil 1212 with potential flow velocity distributions.

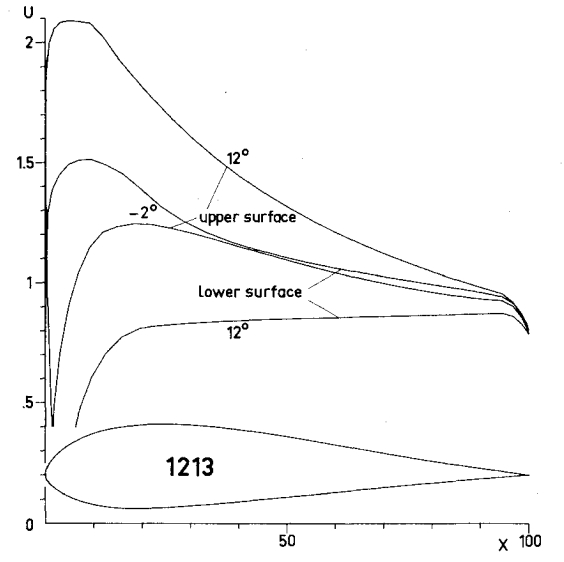

Fig. 13 Airfoil 1213 with potential flow velocity distributions.

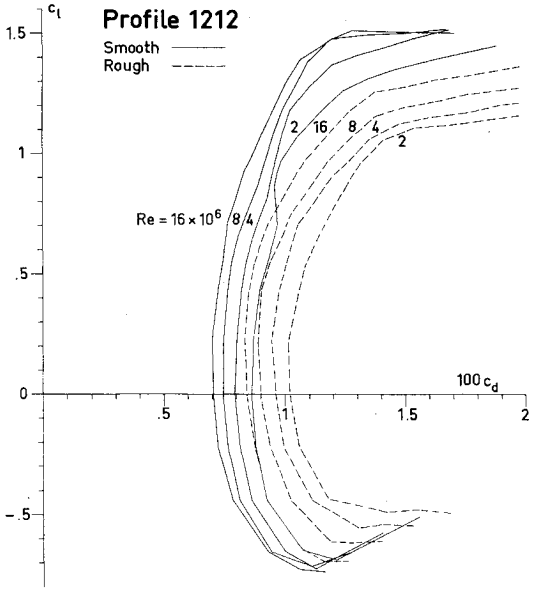

Fig. 12 $c_d - c_l$ polars for airfoil 1212.

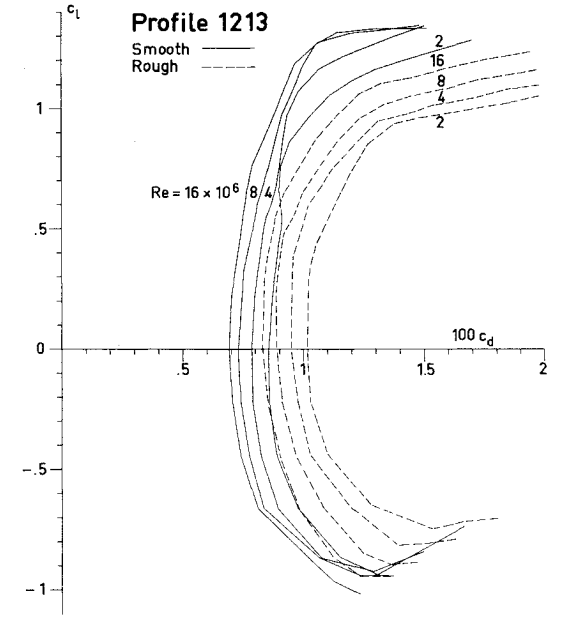

Fig. 14 $c_d - c_l$ polars for airfoil 1213.

The most important result is that the increased thickness has almost no effect on the drag coefficients. This is due to the fact that the suction peak at the lower surface for $\alpha = 2$ deg is not as high as for airfoil 1210. Additionally, for rough conditions the larger region of favorable pressure gradient allows a slightly larger region of laminar flow near the stagnation point. This modification clearly shows that this kind of turbulent airfoil should be thicker in order to reduce weight and wing area.

The next modification is shown in Figs. 11 and 12. It could be more important to have a lower moment coefficient at cruise conditions rather than a high maximum lift coefficient for the unflapped airfoil. It is very easy to shift all velocity specifications to angles of attack which are 2 deg smaller. The profile 1212 specified in this manner has 17.7% thickness and a zero lift moment coefficient of $c_{m_0} = -0.065$, and for cruise conditions, a very small pressure difference between the two sides near the trailing edge. The upper side is nearly straight from the trailing edge up to about $x = 60\%$. Further, the computer drag polars are shifted downwards as compared to those of profile 1211. But the maximum lift coefficient of the flapped airfoil will be large due to the very blunt leading edge.

The latter fact is also true for airfoil 1213, shown in Figs. 13 and 14. The angles of attack for the velocity specifications were reduced by another two degrees. The thickness is now 17.4%, the moment coefficient is $c_{m_0} = -0.021$. There is almost no load at the trailing edge for cruise conditions, and the lower surface can be considered as a straight line between the trailing edge and $x = 50\%$.

Tables showing the coordinates, thicknesses, moment coefficients, and angles of zero lift (β) for all airfoils presented here are available from the author.

V. Conclusions

The profiles discussed in this paper have to be considered as examples. They combine simple shapes with low moment coefficients, low trailing-edge loading, and high flap-down maximum lift. The philosophy is that, without smooth surfaces, a small region of steep favorable pressure gradient is better than a long region of small gradient. In this steep-gradient region the flow remains laminar to a certain degree even for rough surfaces. There, it is at least easier to maintain laminar flow than for approximately constant pressure. If the wing is smooth for only 6% of the lower and 12% of the

upper surface, the "smooth" drag polar will almost be reached. Since most planes have such a smooth leading edge, the advantages of the smooth wing ($r=0$) will be reached frequently. They are equally important for maximum lift and for minimum drag.

In the nomenclature of the NACA 6 series, the airfoils presented here would be characterized by a low second digit and a high index, for example 61_{12}, although exactly constant pressure cannot be obtained for any angle of attack. Of course, there is a steady transition from these new profiles to those with long laminar areas. Depending on Reynolds number, roughness degree, wing loading, engine power and so on, every plane needs another profile. But it is easy to tailor such airfoils for every requirement. The required computing time including the calculation of eight drag polars is less than 30 seconds on a CD 6600 computer.

Some uncertainty is due to the transition criterion and the roughness degree being used. Further developments should be supplemented by experiments, especially by very simple free-flight transition measurements. This would allow a better approach to obtain optimum airfoils for all construction conditions and different layouts of a plane. It might pay off to again extend the region of laminar flow. So far, use of the presented profiles contains no risk and will certainly allow some improvement of the general-aviation airplanes.

Acknowledgment

Most of the computations needed for this paper were made during a visit to the U. S. Air Force Academy, Colorado Springs, in November 1975. The help of Col. Daley, Capt. Smith, and Mrs. A. Hall is appreciated.

References

Eppler, R., "Stand und Aussichten des deutschen Leichtflugzeugbaus," *Jahrbuck 1968 der DGLR*, pp. 93-99.

[2] Raspet, A. and Lambros, G., "Flight Research on a Personal Type of Airplane," *Research Reviews*, Office of Naval Research, Dept. of the Navy, Washington, D. C., April 1954, pp. 12-17.

[3] Eppler, R., "Laminarprofile für Reynoldszahlen größer als 4.10^6," *Ingenieur-Archiv*, Vol. 38, 1969, pp. 232-240.

[4] McGhee, R. J. and Beasley, W. J., "Low Speed Aerodynamic Characteristics of a 17-Percent Thick Airfoil Section Designed for General Aviation Applications," NASA TN D-7428, 1973.

[5] Stevens, W. A., Goradia, S. H., and Braden, J. A., "Mathematical Model for Two-Dimensional Multi-Component Airfoils in Viscous Flow," NASA CR-1841, 1971.

[6] Eppler, R., "Direkte Berechnung von Tragflügelprofilen aus der Druckverteilung," *Ingenieur-Archiv*, Vol. 25, 1957, pp. 32-57.

[7] Eppler, R. "Über die Entwicklung moderner Tragflügelprofile," *De Ingenieur*, Vol. 77, 1965, pp. L15-L21.

[8] Miley, S. J., "An Analysis of the Design of Airfoil Sections for Low Reynolds Numbers," Ph.D. Thesis, Mississippi State University, 1972.

[9] Eppler, R., "Praktische Berechnung laminarer und turbulenter Absauge-Grenzschichten," *Ingenieur-Archiv*, Vol. 32, 1963, pp. 221-245.

[10] Van Ingen, J. L., "Theoretical and Experimental Investigations of Incompressible Laminar Boundary Layers with and without Suction," Dept. of Aeronautical Engineering, University of Technology, Delft, Rept. VTH-124, 1965.

[11] Horton, H. P., "A Semi-Empirical Theory for the Growth and Bursting of Laminar Separation Bubbles," Aeronautics Research Council, CP 1073, 1967.

[12] Wortmann, F. X., "Experimentelle Untersuchungen an neuen Laminarprofilen für Segellfugzeuge und Hubschrauber," *Zeitschrift für Flugwisschaften*, Vol. 5, 1957, pp. 228-243.

[13] Eppler, R., "Beiträge zu Theorie und Anwendung der unstetigen Strömungen," *Journal of Rational Mechanics and Analysis*, Vol. 3, 1954, pp. 591-644.

[14] Squire, H. B. and Young, A. D., "The Calculation of the Profile Drag of Aerofoils," Aeronautics Research Council, MR 1838, 1938.

[15] Betz, A., "Ein Verfahren zur direkten Ermittlung des Profilwiderstandes," *Zeitschrift für Flugtechn. und Motorluftschiffahrt*, Vol. 16, 1925, pp. 42-44.

[16] Peterson, J. B. Jr. and Chen, A. W., "Design Procedure for Low-Drag Subsonic Airfoils," NASA TEC BRIEF, p. 75-10256, 1975.

[17] Abbott, I. H., v. Doenhoff, A. E., and Stivers, L. S., "Summary of Airfoil Data," NACA Rept. 824, 1945.

[18] Liebeck, R. H., "On the Design of Subsonic Airfoils for High Lift," AIAA Paper 76-406, AIAA 9th Fluid and Plasma Dynamics Conference, 1976.

[19] Stratford, B. S., "An Experimental Flow with Zero Skin Friction Throughout its Region of Pressure Rise," *Journal of Fluid Mechanics*, Vol. 5, 1959, pp. 17-35.

[20] Wortmann, F. X., "Ein Beitrag zum Entwurf von Laminarprofilen für Segelflugzeuge und Hubschrauber," *Zeitschrift für Flugwisschaften*, Vol. 3, 1955, pp. 333-345.

[21] Pierpont, K., personal communication, NASA Langley Research Center, Oct. 1975.